Proceedings of the 2006 IEEE
Conference on Computer Aided Control Systems Design
Munich, Germany, October 4-6, 2006

Joint Space Controller Design for Electrohydraulic Servos

Ioannis Davliakos, Athanassios Zafiris, and Evangelos Papadopoulos, *Senior Member, IEEE*

Abstract—**This paper focuses on the joint space control of mechanical systems with electrohydraulic servos. Using mechanism inverse kinematics, desired Cartesian trajectories yield desired actuator trajectories, which are fed to a novel model-based controller. Rigid body equations of motion and hydraulics dynamics, including friction and servovalve models are employed. The developed feedback controller uses the system dynamic and hydraulic model to yield servovalve currents. As an example, the developed controller is applied to a single degree-of-freedom (dof) servomechanism. Identification procedures employed in estimating the physical parameters of the experimental single dof servomechanism are discussed. In contrast to other approaches, here, force, pressure or acceleration feedback is not required. Simulations with typical desired trajectory inputs are presented and a good performance of the controller is obtained.**

I. Introduction

MODERN hydraulic technology combining both hydraulics science and servo control technology, has provided a new thrust to hydraulics applications. Hydraulics are preferred to electromechanical drives in some industrial and mobile applications, because of their ability to produce large forces at high speeds, their high durability and stiffness, and their rapid response [1].

Hydraulic systems differ from electromechanical ones, in that the force or torque output is not proportional to actuator current and therefore, hydraulic actuators cannot be modeled as force/ torque sources. As a result, controllers that have been designed for robot control, assuming the capability of setting actuator force/ torque, cannot be used here. To use such controllers, the model of a hydraulic actuator drive should be approached as a compound resistance [2].

Control techniques are used to compensate for the nonlinearities of electrohydraulic servosystems. Nonlinear adaptive control techniques for hydraulic servosystems have been proposed by researchers assuming linearization [3] and backstepping [4], approaches. Further, an adaptive controller for high bandwidth servovalves has been studied and achieved in [5]. This controller has been developed for a system that uses full-state feedback for simultaneous on-line parameter identification and tracking control.

A model-based, feedforward-feedback impedance control scheme of hydraulic servosystems for high-performance hydraulic joints has been proposed, in which an impedance filter adjusts the desired trajectory according to a prescribed behaviour in free space and in contact [6]. Similar work has been presented in [7], where a position-based impedance controller for an industrial hydraulic manipulator is developed. A tracking controller for electrohydraulic servosystems has been developed [8], including a fast model-based force tracking loop. Also, a tracking controller of an electrohydraulic manipulator [9], which is based on a friction compensating control strategy, including acceleration feedback control, has been studied.

Most of the previous work associated with parameter estimation and system identification has been focused on electrohydraulic servoactuators [10]-[14]; the identification of a highly nonlinear hydraulic positioning actuator, using discrete-time linear models has been discussed in [11]. Modeling and experimental identification of friction has been carried out for an asymmetric hydraulic cylinder, where friction was found to be highly dependent on the direction of piston motion [12]. Modeling and parameter estimation for the electrohydraulic actuation system of an articulated forestry machine has been studied in [13]. A combined scheme of identification and robust control for rotary hydraulic actuators [14] has been developed, using a dynamic feedback linearizing inner loop, cascaded with an optimal $l_1 - H_\infty$ feedback outer loop.

In this paper, a joint space controller of mechanical systems with electrohydraulic servo-drive is developed. Desired Cartesian trajectories yield the desired actuator trajectories using mechanism inverse kinematics that are fed to a novel model-based controller. Dynamic models of low complexity, including friction and servovalve models, are employed that describe the salient dynamics of basic electrohydraulic components. The control law design uses the system dynamic and hydraulic model to yield servovalve currents. In contrast to other approaches, here, force, pressure or acceleration feedback is not required. An example single degree-of-freedom (dof) servomechanism is studied, for which identification procedures employed in estimating its physical parameters are presented. Model validation studies show good agreement between model predictions and experiments. Simulations with typical desired trajectory inputs are presented.

Manuscript received February 9, 2006. Support by the EPAN Cooperation Program 4.3.6.1 (Greece-Poland) of the Hellenic General Secretariat for Research and Technology and the NTUA Senator Committee of Basic Research Programme "Protagoras", R.C. No. 10, is acknowledged.

I. Davliakos is with the National Technical University of Athens, Greece (e-mail: gdavliak@central.ntua.gr).

A. Zafiris is with the National Technical University of Athens, Greece (e-mail: mcp04207@central.ntua.gr).

E. Papadopoulos is with the National Technical University of Athens, Greece (corresponding author phone: +(30)210-772-1440; fax: +(30)210-772-1455; e-mail: egpapado@ central.ntua.gr).

II. System Modeling

In this section, the dynamic modelling of high performance electrohydraulic servocylinders is presented briefly. An electrohydraulic servosystem consists of a servomechanism, including a servovalve, a servoactuator, a controller, a mechanical load, hydraulic hoses and a hydraulic power supply. Next, simple models of major components are described.

A full servosystem model includes the moving mass equation of motion. This system provides a relation between the actuator torques/forces and the resulting motion. The servomechanism equation of motion is given by,

$$\mathbf{M}(\boldsymbol{q})\ddot{\boldsymbol{q}} + \boldsymbol{V}(\boldsymbol{q},\dot{\boldsymbol{q}}) + \boldsymbol{G}(\boldsymbol{q}) + \boldsymbol{F}_{fr}(\dot{\boldsymbol{q}}) = \boldsymbol{\tau} \tag{1}$$

where $\boldsymbol{q}$ is the $n\times 1$ vector of generalized coordinates, $\mathbf{M}(\boldsymbol{q})$ is the $n\times n$ positive definite mass matrix, the $\boldsymbol{V}(\boldsymbol{q},\dot{\boldsymbol{q}})$ vector represents forces/torques arising from centrifugal and Coriolis forces, the $n\times 1$ vector $\boldsymbol{G}(\boldsymbol{q})$ represents torques due to gravity, $\boldsymbol{F}_{fr}(\dot{\boldsymbol{q}})$ is the $n\times 1$ vector of the forces/ torques due to friction including viscous and Coulomb friction vector, and $\boldsymbol{\tau}$ is the $n\times 1$ vector of actuator joint torques.

An ideal single rod hydraulic cylinder is described by,

$$Q_1 = A_1\dot{x}_p, \quad Q_2 = A_2\dot{x}_p \tag{2a}$$

$$p_1A_1 - p_2A_2 = F_p \tag{2b}$$

where Q_1, Q_2 are the flows through its two chamber ports, p_1, p_2 are the chamber pressures, A_1 is the piston side area, A_2 is the rod side area, x_p is the piston displacement and F_p is the piston output force. A real cylinder model also includes chamber oil compressibility, friction and other effects. However, these can be neglected at an initial stage. In the case of an ideal hydraulic cylinder with a double rod, the two areas A_1 and A_2 are equal and therefore, (2b) is simplified further.

A typical hydraulic servovalve consists of four symmetric and matched servovalve orifices making up a four-legged flow path of four nonlinear resistors, modulated by the input voltage, see Fig. 1(a). Thereby, the servovalve is modeled as the hydraulic equivalent of a Wheatstone bridge, see Fig. 1(b). When flow passes through the orifices 1 and 3 (main path $P\to A\to B\to T$), flow leakages exist in the valve orifices 2 and 4. Respectively, when flow passes through the path $P\to B\to A\to T$, flow leakages exist in the valve orifices 1 and 3. This model is described by

$$Q_{v1} = f_1(i)\sqrt{p_s - p_1}, \quad Q_{v3} = g_1(i)\sqrt{p_2 - p_T} \tag{3a}$$

$$Q_{v2} = f_2(i)\sqrt{p_s - p_2}, \quad Q_{v4} = g_2(i)\sqrt{p_1 - p_T} \tag{3b}$$

where p_s and p_T are the power supply and return pressure of the servosystem, respectively, i is the servovalve motor current (control command), $f_1(i)$, $f_2(i)$, $g_1(i)$ and $g_2(i)$ are nonlinear functions in the servovalve motor current. Because of servovalve symmetry, the current functions are given by,

$$f_1(i) = g_1(i) = f_2(-i), \quad f_2(i) = g_2(i) = f_1(-i) \tag{4}$$

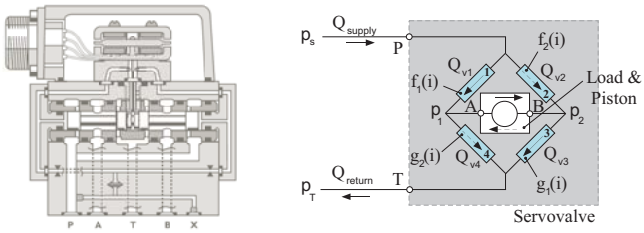

(a) (b)

Fig. 1. (a) A drawing of a real servovalve, (b) Schematic model of servovalve.

A good approximation is to assume that current functions are linear functions in the input current, when flow passes through the main path and constants, when flow passes through the leakage flow path. For instance, when $i > 0$, the main flow path passes through the orifices 1 and 3 and the functions are given by,

$$f_1(i) = g_1(i) = K_1 i + K_{0,1} \tag{5a}$$

$$f_2(i) = g_2(i) = K_{0,1} \tag{5b}$$

where K_1 and $K_{0,1}$ are constants, which correspond to the main and leakage valve flow path.

Further, neglecting leakages flows, the flows through the orifices of the servovalve described in (3a), are equal to the flows through the cylinder chamber ports, see (2a),

$$Q_{v1} = Q_1 = A_1\dot{x}_p, \quad Q_{v3} = Q_2 = A_2\dot{x}_p \tag{6}$$

Hydraulic hoses of an electrohydraulic servosystem are modeled as compressible hydraulic lines. The equations that describe the hose dynamics are given by,

$$p_{l,in} - p_{l,m} = R\,Q_{l,in}, \quad \dot{Q}_{l,out} = (p_{l,m} - p_{l,out})/I \tag{7a}$$

$$\dot{p}_{l,m} = (Q_{l,in} - Q_{l,out})/C \tag{7b}$$

where $p_{l,in}$, $p_{l,out}$ and $p_{l,m}$ are the hose pressures at its input, output and a middle point respectively, $Q_{l,in}$, $Q_{l,out}$ are the flows through the hose at its input and output correspondingly, and the hose parameters R, I, C are the resistance, inertance and capacitance, respectively of the hydraulic line, [15], [16].

Hydraulic power units regulate and supply the required hydraulic power of the servo plant. Hydraulic pumps are usually constant pressure piston pumps, driven by an induction electric motor. Further, hydraulic supplies may include accumulators for filtering pressure pulsations from

the pump, but also for allowing the use of smaller rating pumps by providing additional flow when needed.

The hydraulic and load dynamic response can be described by integrated system equations derived using a systems approach, such as the Linear Graph [15] or Bond Graph methods [16]. To this end, one needs to provide expressions transforming pressure differences to forces, see (2b), and velocities to flows, see (2a). In general, the integrated hydraulic and mechanical load dynamics are described by nonlinear equations,

$$\begin{aligned} \dot{\boldsymbol{x}} &= \boldsymbol{f}(\boldsymbol{x}) + \boldsymbol{g}(\boldsymbol{x})\boldsymbol{u} \\ \boldsymbol{y} &= \boldsymbol{h}(\boldsymbol{x}), \qquad \boldsymbol{x} = \boldsymbol{x}(t_0) = \boldsymbol{x}(\boldsymbol{0}) \end{aligned} \tag{8}$$

where $\boldsymbol{x}$ is a state column vector, $\boldsymbol{x_0}$ is the initial state column vector for initial time $t_0 = 0$, $\boldsymbol{u}$ is the input column vector, $\boldsymbol{y}$ is the output column vector and, $\boldsymbol{f}(\boldsymbol{x})$, $\boldsymbol{g}(\boldsymbol{x})$ and $\boldsymbol{h}(\boldsymbol{x})$ are nonlinear functions.

III. Controller Design

To control an n dof electrohydraulic mechanism, such as a 6-dof Stewart platform [17], in operational (Cartesian) space, first, manipulator inverse kinematics is solved to transform motion requirements from operational-space into the joint-space. Then, a joint space control scheme is designed that allows tracking of the reference inputs.

In electromechanical systems, the force acting on moving masses is proportional to actuator current. This simplifies their control laws and allows one to achieve second order error dynamics converging exponentially to zero. However, a simple relationship between force and current does not exist in electrohydraulic systems. Despite of this, we are interested in studying whether such an n dof system can be described by error dynamics such as

$$\ddot{\boldsymbol{e}} + \mathbf{K}_{\mathrm{v}}\dot{\boldsymbol{e}} + \mathbf{K}_{\mathrm{p}}\boldsymbol{e} = \boldsymbol{0} \tag{9}$$

where $\boldsymbol{e} = \boldsymbol{q}_{des} - \boldsymbol{q}$ is the $n \times 1$ vector position error of the actuator displacements, $\boldsymbol{q}_{des}$ is the $n \times 1$ desired vector of the actuator displacements, and $\mathbf{K}_{\mathrm{p}}$ and $\mathbf{K}_{\mathrm{v}}$ are $n \times n$ diagonal matrixes, which represent the control gains of the system and are given by,

$$\mathbf{K}_{\mathrm{p}} = diag\{\omega_1^2, ..., \omega_j^2, ..., \omega_n^2\} \tag{10a}$$

$$\mathbf{K}_{\mathrm{v}} = diag\{2\zeta_1\omega_1, ...2\zeta_j\omega_j, ..., 2\zeta_n\omega_n\} \tag{10b}$$

where ω_j and ζ_j, $j = 1, 2, ..., n$, are the n actuators closed-loop natural frequency and damping respectively.

Using (3), (5) and (6), the servocylinder chamber pressures are computed,

$$p_1\big|_j = [\,p_s - A_1^2 (K_1 i + K_{0,1})^{-2} \dot{x}_p^2\,]\big|_j, \quad j = 1, 2, ..., n \tag{11a}$$

$$p_2\big|_j = [\,p_T + A_2^2 (K_1 i + K_{0,1})^{-2} \dot{x}_p^2\,]\big|_j, \quad j = 1, 2, ..., n \tag{11b}$$

Substituting (11) in (2b), the hydraulic forces of the servoactuators are computed as,

$$\begin{aligned} [\,p_1 A_1 - p_2 A_2\,]\big|_j = {} & [\,p_s A_1 - p_T A_2\,]\big|_j - \\ & [\,(A_1^3 + A_2^3)(K_1 i + K_{0,1})^{-2} \dot{x}_p^2\,]\big|_j, \quad j = 1, 2, ..., n \end{aligned} \tag{12}$$

In (12), i_j is the control input for the j[th] valve /actuator and $[\,p_1 A_1 - p_2 A_2\,]\big|_j$ is the resulting actuator force. However, (12) is also function of the velocity of the actuators, $\dot{x}_{p,j}$. Substituting (12) in the system equation of motion, see (1), the following equations of motion are derived,

$$\begin{aligned} & \mathbf{M}(\boldsymbol{q})\ddot{\boldsymbol{q}} + \boldsymbol{V}(\boldsymbol{q}, \dot{\boldsymbol{q}}) + \boldsymbol{G}(\boldsymbol{q}) + \boldsymbol{F}_{fr}(\dot{\boldsymbol{q}}) = \\ & \qquad \begin{bmatrix} [\,p_s A_1 - p_T A_2 - (A_1^3 + A_2^3)(K_1 i + K_{0,1})^{-2} \dot{x}_p^2\,]\big|_1 \\ \cdots \\ [\,p_s A_1 - p_T A_2 - (A_1^3 + A_2^3)(K_1 i + K_{0,1})^{-2} \dot{x}_p^2\,]\big|_n \end{bmatrix} \end{aligned} \tag{13}$$

Solving (13) for the input commands, i_j, $j = 1, 2, ..., n$, the components of the valve current vector $\boldsymbol{i} = (i_1, i_2, ..., i_n)^{\mathrm{T}}$ are computed as,

$$\begin{aligned} i_j = {} & [\,\dot{x}_p K_1^{-1} / \sqrt{(p_s A_1 - p_T A_2 - \langle F \rangle)(A_1^3 + A_2^3)^{-1}}\,]\big|_j - \\ & [\,K_{0,1} K_1^{-1}\,]\big|_j, \quad j = 1, 2, ..., n \end{aligned} \tag{14}$$

where $\langle F \rangle\big|_j$ represents the j^{th} element of the column vector $\mathbf{M}(\boldsymbol{q})\ddot{\boldsymbol{q}} + \boldsymbol{V}(\boldsymbol{q}, \dot{\boldsymbol{q}}) + \boldsymbol{G}(\boldsymbol{q}) + \boldsymbol{F}_{fr}(\dot{\boldsymbol{q}})$.

Further, assuming that (9) have been achieved, this equation is solved for $\ddot{\boldsymbol{q}}$ which is substituted in the elements $\langle F \rangle\big|_j$. Then, the $\langle F \rangle\big|_j$ elements are given by,

$$\begin{aligned} \langle F \rangle\big|_j = {} & \mathbf{M}(\boldsymbol{q}) \cdot (\ddot{\boldsymbol{q}}_{des} + \mathbf{K}_{\mathrm{v}}\dot{\boldsymbol{e}} + \mathbf{K}_{\mathrm{p}}\boldsymbol{e}) \\ & + \boldsymbol{V}(\boldsymbol{q}, \dot{\boldsymbol{q}}) + \boldsymbol{G}(\boldsymbol{q}) + \boldsymbol{F}_{fr}(\dot{\boldsymbol{q}}) \end{aligned} \tag{15}$$

Finally, the servovalve current vector, the elements of which are given in (14), describes the joint space control law scheme for an n dof electrohydraulic servosystem. Note that force, pressure or acceleration feedback is not required. The control law only requires feedback of both the position and velocity errors, and includes the mechanism dynamics and the servovalve model.

Substituting (14) in (1), an equation of the form of (9) results, which demonstrates the stability of the system. The system control law is illustrated schematically in Fig. 2.

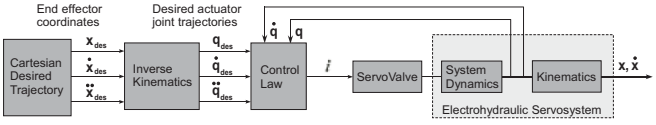

Fig. 2. Schematic view of the joint space controller diagram.

IV. ONE–DOF ELECTROHYDRAULIC SERVOMECHANISM

A. Servosystem Modelling

In this section, the dynamic model of one-degree-of-freedom electrohydraulic servomechanism is developed. This servo is to be used as an actuator in a robotic Stewart type mechanism [17], i.e. a six dof closed kinematic chain mechanism consisting of a fixed base and a movable platform with six linear actuators supporting it. The one dof mechanism is illustrated schematically in Fig. 3.

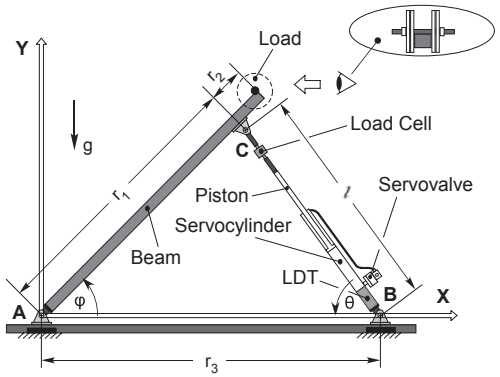

Fig. 3. Schematic view of the one-dof servomechanism model.

The actuator inclination angle θ, and the load angle φ, shown in Fig. 3 can be expressed as function of the displacement of the actuator, x_p. Applying the Lagrange formulation, the equation of motion is written as,

$$M(x_p)\ddot{x}_p + V(x_p,\dot{x}_p) + G(x_p) + F_{fr}(\dot{x}_p) = F_p \tag{16}$$

where $M(x_p)$ is a positive definite function, which represents the variable apparent mass of the mechanism, as seen by the actuator, $V(x_p,\dot{x}_p)$ contains the Coriolis and centrifugal terms, $G(x_p)$ represents the gravity term, F_p is the force applied to the mechanical load and $F_{fr}(\dot{x}_p)$ is the friction term. The terms $M(x_p)$, $V(x_p,\dot{x}_p)$, $G(x_p)$ and $F_{fr}(\dot{x}_p)$ are given explicitly in [8].

The hydraulics equations of the servomechanism are described by (2)-(7). One of the most important characteristics is the servovalve characteristic, $Q_v - \Delta p_v$. The flow through the cylinder and the piston output force applied to the load are given by (2a) and (2b), correspondingly. The pressure drop at the servovalve is expressed using (3).

The application of continuity and compatibility laws, along with individual elements equations, leads to a set of eight nonlinear first order differential equations, in the form of (8), as follows,

$$\dot{p}_1 = [Q_{l,l1} - Q_{v2} - Q_{v4} - C_{p,in}(p_1 - p_2) - A_1 v_p] C_1^{-1} \tag{17a}$$

$$\dot{p}_2 = [Q_{v2} + Q_{v4} - Q_{l,l2} + C_{p,in}(p_1 - p_2) + A_2 v_p] C_2^{-1} \tag{17b}$$

$$\dot{p}_{C,l1} = [(p_s - p_{C,l1})/R_{l1} - Q_{l,l1}] C_{l1}^{-1} \tag{17c}$$

$$\dot{p}_{C,l2} = [Q_{l,l2} - (p_{C,l2} - p_T)/R_{l2}] C_{l2}^{-1} \tag{17d}$$

$$\dot{Q}_{l,l1} = [p_{C,l1} - p_1 - C_{R1} Q_{v1} |Q_{v1}|] I_{l1}^{-1} \tag{17e}$$

$$\dot{Q}_{l,l2} = [p_2 - p_{C,l2} - C_{R3} Q_{v3} |Q_{v3}|] I_{l2}^{-1} \tag{17f}$$

$$\dot{v}_p = M^{-1}(x_p)[A_1 p_1 - A_2 p_2 - V(x_p,\dot{x}_p) - G(x_p) - F_{fr}(\dot{x}_p)] \tag{17g}$$

$$\dot{x}_p = v_p \tag{17h}$$

where $Q_{l,l1}$, $Q_{l,l2}$ are the flows in hydraulic power and return line correspondingly, $p_{C,l1}$, $p_{C,l2}$ are respectively the pressures of hydraulic power and return line regarding with the lines' capacitances, I_{l1}, R_{l1}, and C_{l1} are the inertance, resistance and capacitance of hydraulic power line respectively, I_{l2}, R_{l2}, and C_{l2} are the inertance, resistance and capacitance of hydraulic return line respectively, C_1, and C_2 are the fluid capacitance in the servoactuator chambers, and $C_{p,in}$ is the internal leakage coefficient of piston.

B. Experimental Identification

The majority of the parameters were identified individually in order to minimize estimation errors. Various types of sensors and devices were used for the experiments. A Moog G761-3004 Series high-performance servovalve was used to control the cylinder flow. Also, a Moog G122-202A1 Series controller was used to measure the piston position, with a built-in MTS analog magnetostrictive transducer (LVDT). WEBTEC LPT-6000 P-N pressure sensors were used to measure hydraulic line pressure and servocylinder headside and rodside pressure. A bilateral HBM U9B strain gauge force cell at the end of the rod provided the load force. Fluid flow was measured using FTI MAG type preamplifier flow meters. The data-acquisition system was based on a National Instruments PCI-6035E board, running in LabView.

Hose parameters. Hydraulic hose parameters, R, I, C are estimated using least squares techniques. The methodology is based on solving the equation,

$$\mathbf{A}\,\mathbf{x} = \mathbf{b} \tag{18}$$

where $\mathbf{A}$, $\mathbf{b}$ are a square matrix and a column vector, respectively function of the measured system variables, and $\mathbf{x}$ is the unknown parameter column vector. The solution of (18) requires the computation of the inverse of $\mathbf{A}$ to yield $\mathbf{x}$. Writing the hydraulic hose dynamics, (7), in the form of (18) results in,

$$\begin{pmatrix} Q_{l,in} & 0 & 0 \\ 0 & \dot{Q}_{l,out} & 0 \\ 0 & 0 & \dot{p}_{l,m} \end{pmatrix} \begin{pmatrix} R \\ I \\ C \end{pmatrix} = \begin{pmatrix} p_{l,in} - p_{l,m} \\ p_{l,m} - p_{l,out} \\ Q_{l,in} - Q_{l,out} \end{pmatrix} \tag{19}$$

For the 1-dof electrohydraulic servomechanism hose with length of 3.5 meters and diameter $3/4''$, four groups of data were collected. The mean values of the resistance, inertance and capacitance were calculated from each group of data

and the final results were obtained as the average of these four mean values. These values were estimated as, $I = 3.75 \times 10^7\,\mathrm{kg/m^4}$, $R = 6.57 \times 10^8\,\mathrm{Ns/m^5}$, $C = 1.072 \times 10^{-12}\,\mathrm{m^5/N}$.

Servovalve. The objective is to estimate the relationship between current input and the valve orifice functions, see (5). These functions, for the main and leakage servovalve path are illustrated in Fig. 4(a). Measurements up to 40% valve opening were achieved, as shown in Fig. 4(a).

Further, Fig. 4(b) displays the plots of the resulting valve flow versus valve pressure drop curve of a main (solid lines) and leakage (dotted lines) servovalve orifice for orifice open 30%, 60% and 100%. This type of curve represents one of the most important servovalve characteristic curves, which was achieved using the valve orifice functions. The servosystem power supply was selected to be $p_s = 110$ bar [18], return pressure is $p_T = 1$ bar and the piston side and rod side area are $A_1 = 2.56 \times 10^{-4}\,\mathrm{m^2}$ and $A_2 = 6.41 \times 10^{-4}\,\mathrm{m^2}$ correspondingly.

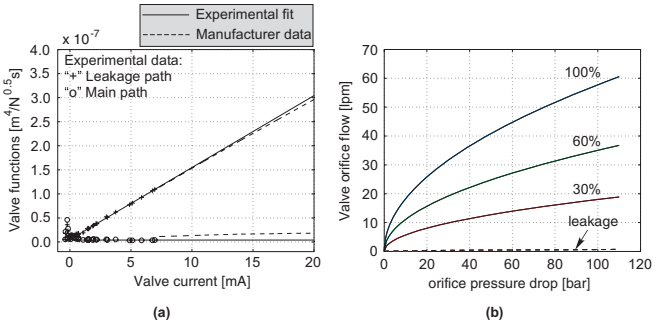

Fig. 4. (a) Valve functions in main and leakage path, (b) Force-velocity diagram for the 1-dof servomechanism.

Friction. Friction between piston and servocylinder has a significant effect on the system response, as predicted by the simulation. Several experiments were performed at different velocities. Fig 5 shows in dotted values the friction force of the servocylinder as a function of piston velocity.

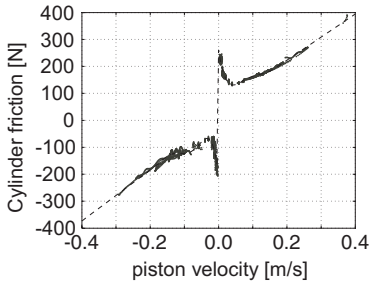

Fig. 5. Hydraulic cylinder friction force vs. piston velocity.

C. Model Validation

To test how well the model can predict system behavior, experiments and simulations were compared. Plots comparing actual and predicted values of the piston displacement and the axial hydraulic force actuation for an input command are shown in Fig. 6. The solid lines correspond to actual measurements and the dotted lines are the predictions using the dynamic and hydraulic model by simulation.

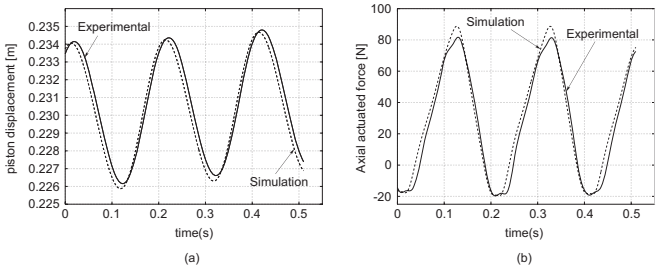

Fig. 6. Actual and predicted histories of (a) the piston displacement and (b) the axial hydraulic force.

D. Control

In this section, the developed control scheme is applied to the single-dof electrohydraulic servomechanism. Following the joint space control strategy of Section III, the control law for the 1-dof servomechanism is, see (14),

$$i = \dot{x}_p K_1^{-1} / \sqrt{(p_s A_1 - p_T A_2 - F) \cdot (A_1^3 + A_2^3)^{-1}} - K_{0,1} K_1^{-1} \qquad (20)$$

where F is given by,

$$F = M(x_p) \cdot (\ddot{x}_{p,des} + K_v \dot{e} + K_p e) + V(x_p, \dot{x}_p) + G(x_p) + F_{fr}(\dot{x}_p) \qquad (21)$$

where $e = x_{p,des} - x_p$ is the position error of the servo-actuator displacement, and $x_{p,des}$ is the desired position.

A custom-designed benchmark setup shown in Fig. 7(a) was built at the NTUA to test the proposed controller. The particular design of the setup allows for easy changes in the static and dynamic components of the inertial load, driven by the actuator. This is achieved by varying the angle of the cylinder with respect to the horizontal and by changing the cylinder inertia, by adding or removing load's weight.

Currently, a real-time controller written in C and running under QNX (a real-time operating system) is being developed. The PID control section of the card is by passed and the Moog amplifier card is only used for reading feedback measurements and for sending the appropriate control voltages to the servoamplifier. The servoamplifier in turn will send appropriate currents to the servovalve, see Fig 7(b).

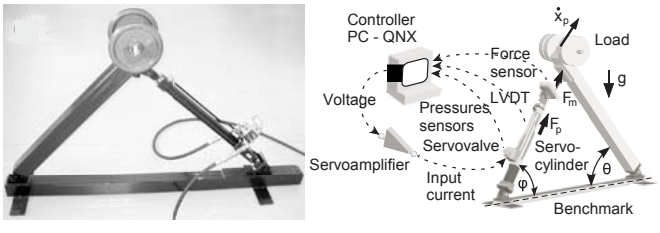

Fig. 7. (a) The real driven load and its servomechanism, (b) Schematic of control system setup and benchmark.

V. SIMULATION RESULTS

The tracking performance of the controller is evaluated on the full hydraulic servosystem, described by (17a-h), using Matlab/Simulink. The estimated system parameters include expressions, as, $m_p a_p^2 = 61.15\,\text{kgm}^2$, $I_b + m_b a_b^2 = 11.93\,\text{kgm}^2$ $I_{cyl} + I_p + m_{cyl} a_{cyl}^2 + m_p a_p^2 = 61.15\,\text{kgm}^2$, $b_{pin} = 1.44 \times 10^{-7}\,\text{Ns}$ and $m_p = 5\,\text{kg}$, where I_b, I_{cyl}, I_p are the beam, cylinder and piston moments of inertia, about their centers of masses respectively, m_b, m_{cyl}, m_p are the masses of beam, cylinder and piston respectively, b_{pin} is the viscous torque friction coefficient of the pin joints, and a_b, a_{cyl}, a_p are the distances of the centers of masses of beam, cylinder and piston from the joints A, B and C correspondingly. Geometrical parameters include parameters such as $r_1 = 1.04\,\text{m}$, $r_2 = 0.08\,\text{m}$ and $r_3 = 1.64\,\text{m}$, see Fig. 3.

Simulation runs were obtained using a number of desired trajectories. As an example, Fig. 8 shows typical results with load mass $m = 60\,\text{kg}$, natural frequency $\omega = 10\pi$ rad/s, and critical system damping $\zeta = 1$. The piston displacement and velocity responses and their error histories, the input signal, and chamber pressures histories are shown in Fig. 8. The position errors converge to zero, as expected, with a settling time $t_s = 6/\omega = 0.19\,\text{s}$.

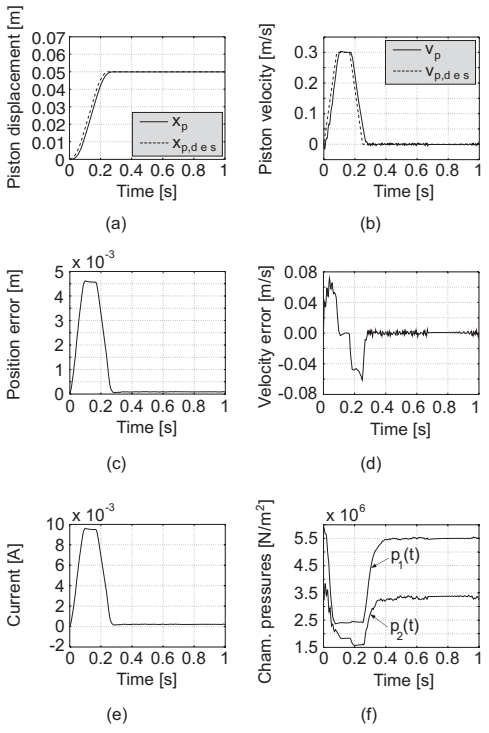

Fig. 8. Simulation results. (a) Piston displacement response, (b) Piston velocity response, (c) position error, (d) velocity error, (e) Input signal, (f) Chamber pressures histories.

VI. CONCLUSION

In this paper, a joint space controller of mechanical systems with electrohydraulic servo-drive was developed. Using mechanism inverse kinematics, the desired Cartesian trajectories yielded desired actuator trajectories. Dynamic models of low complexity, including friction and servovalve models, were employed that describe the salient dynamics of basic electrohydraulic components. The control law design based on the system dynamic and hydraulic model to yield servovalve currents. In contrast to other approaches, here, force, pressure or acceleration feedback was not required. An example 1-dof servomechanism was studied and identification procedures employed in estimating the physical parameters of the experimental servomechanism were presented. Model validation studies showed good agreement between model predictions and experiments. Simulation results of typical trajectory commands showed very good performance. The proposed methodology can be extended to electrohydraulic serial or closed-chain manipulators and simulators.

REFERENCES

[1] M. Jelali, and A. Kroll, *Hydraulic Servo-systems. Modelling, Identification and Control*, Springer, 2003.

[2] H. E. Merritt, *Hydraulic Control Systems*, J. Wiley, 1967.

[3] D. Garagic, and K. Srinivasan, "Application of Nonlinear Adaptive Control Techniques to an Electrohydraulic Velocity Servo-mechanism," *IEEE Trans. on Control Systems Tech.*, vol. 12, No. 2, pp. 303–314, 2004.

[4] M. R. Sirouspour, and S. E. Salcudean, "Nonlinear Control of Hydraulic Robots," *IEEE Trans. on Robotics and Automation*, vol. 17, No. 2, pp. 173–182, 2001.

[5] J. E. Bobrow, and K. Lum, "Adaptive, High Bandwidth Control of a Hydraulic Actuator," *Trans. of the ASME*, vol. 118, pp. 714–720, 1996.

[6] I. Davliakos, and E. Papadopoulos, "Development of a Model-Based Impedance Controller for Electrohydraulic Servos," *Proc. Int. Conf. on Robotics and Applications*, Cambridge, USA Oct. 31-Nov. 2, 2005.

[7] B. Heinrichs, N. Sepehri, and A. B. Thornton-Trump, "Position-Based Impedance Control of an Industrial Hydraulic Manipulator," *IEEE Control Systems,* pp. 46-52, February 1997.

[8] I. Davliakos, and E. Papadopoulos, "Development of a Model-Based Nested Controller for Electrohydraulic Servos," *Proceedings 13th Mediterranean Conference on Control and Automation,* Limassol, Cyprus, pp. 107–112, June 27-29, 2005.

[9] S. Tafazoli, C. W. de Silva, and P. D. Lawrence, "Tracking Control of an Electrohydraulic Manipulator in the Presence of Friction," *IEEE Trans. on Control Systems Tech.*, vol. 6, No. 3, pp. 401–411, 1998.

[10] G. A. Sohl, and J. E. Bobrow, "Experiments and Simulations on the Nonlinear Control of a Hydraulic Servosystem," *IEEE Trans. on Control Systems Tech.*, vol. 7, No. 2, pp. 238–247, 1999.

[11] K. Ziaei, and N. Sepehri, "Modeling and Identification of Electro-hydraulic Servos," *Mechatronics,* vol. 10, pp. 761-772, 2000.

[12] A. Bonchis, P. I. Corke, and D. C. Rye, *Proc. 1999 IEEE Int. Conf. on Robotics & Automation*, Detroit, Michigan, pp. 1746–1751, 1999.

[13] E. Papadopoulos, B. Mu, and R. Frenette, "On Modeling, Identification and Control of a Heavy-duty Electrohydraulic Harvester Manipulator," *IEEE/ASME Transactions on Mechatronics*, vol. 8, No 2, pp. 178-187, June 2003.

[14] M. Namvar, and F. Aghili, "A Combined Scheme for Identification and Robust Torque Control of Hydraulic Actuators," *J. of Dyn. Systems, Measurement and Control*, vol. 125, pp. 595–606, 2003.

[15] D. Rowell, and D. N. Wormley, *System Dynamics: An Introduction*, Copyright 1994.

[16] R. Rosenberg, and D. Karnopp, *Introduction to Physical System Dynamics*, McGraw Hill, New York, 1983.

[17] D. Stewart, "A platform with six degrees of freedom," *Proc. of the IMechE*, Vol. 180, Pt. 1, No 15, 1965-66, pp. 371-385.

[18] E. Papadopoulos, and I. Davliakos, "A Systematic Methodology for Optimal Component Selection of Electrohydraulic Servosystems," *International Journal of Fluid Pow*er, vol. 5, No. 2, pp. 15-24, 2004.